

See discussions, stats, and author profiles for this publication at: <https://www.researchgate.net/publication/23711155>

Metal Tetrphosphonate "Wires" and Their Corrosion Inhibiting Passive Films

ARTICLE *in* INORGANIC CHEMISTRY · FEBRUARY 2009

Impact Factor: 4.76 · DOI: 10.1021/ic802032y · Source: PubMed

CITATIONS

24

READS

21

4 AUTHORS, INCLUDING:



[Konstantinos D Demadis](#)

University of Crete

142 PUBLICATIONS 3,654 CITATIONS

SEE PROFILE



[Raphael G Raptis](#)

Florida International University

142 PUBLICATIONS 2,492 CITATIONS

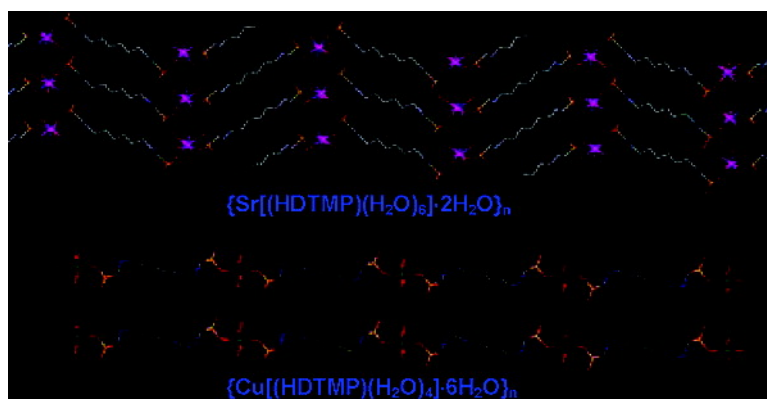
SEE PROFILE

Metal Tetraphosphonate “Wires” and Their Corrosion Inhibiting Passive Films

Konstantinos D. Demadis, Eleni Barouda, Raphael G. Raptis, and Hong Zhao

Inorg. Chem., **2009**, 48 (3), 819-821 • DOI: 10.1021/ic802032y • Publication Date (Web): 29 December 2008

Downloaded from <http://pubs.acs.org> on January 27, 2009



More About This Article

Additional resources and features associated with this article are available within the HTML version:

- Supporting Information
- Access to high resolution figures
- Links to articles and content related to this article
- Copyright permission to reproduce figures and/or text from this article

[View the Full Text HTML](#)



ACS Publications
High quality. High impact.

Metal Tetraphosphonate “Wires” and Their Corrosion Inhibiting Passive Films

Konstantinos D. Demadis,* Eleni Barouda, Raphael G. Raptis,[†] and Hong Zhao[‡]*Crystal Engineering, Growth and Design Laboratory, Department of Chemistry, University of Crete, Voutes Campus, Heraklion, Crete GR-71003, Greece*

Received October 23, 2008

Herein, we describe the preparation and characterization of five new divalent metal tetraphosphonates, M-HDTMP [$M = \text{Mg}^{2+}$, Ca^{2+} , Sr^{2+} , Ba^{2+} , and Cu^{2+} ; HDTMP = hexamethylenediaminetetrakis(methylenephosphonate) dianion]. Materials $\{\text{Sr}[(\text{HDTMP})(\text{H}_2\text{O})_6] \cdot 2\text{H}_2\text{O}\}_n$ (**1**), $\{\text{Ba}[(\text{HDTMP})(\text{H}_2\text{O})_6] \cdot 2\text{H}_2\text{O}\}_n$ (**2**), and $\{\text{Cu}[(\text{HDTMP})(\text{H}_2\text{O})_4] \cdot 6\text{H}_2\text{O}\}_n$ (**3**), as well as $(\text{en})(\text{HDTMP}) \cdot 2\text{H}_2\text{O}$ ($\text{en} = \text{ethylenediammonium cation}$) have been structurally characterized. Structures depend on the coordination requirements of the M^{2+} center and waters of crystallization content. The formation and characterization of effective anticorrosion passive films of M-HDTMP ($M = \text{Sr}^{2+}$ and Ba^{2+}) are also reported.

The research area of coordination polymers is by now an established field of chemical science.¹ The combination of metal centers or clusters with a phalanx of polyfunctional ligands can create limitless possibilities for inorganic–organic hybrid solids.² Factors that affect the fate of end product(s) are multiple: nature of M^{n+} , coordination number, nature and number of functional groups and ligand charge, different coordinating moieties, and, naturally, process variables (temperature, solvent, pressure, etc.).^{2,3} Phosphonates find widespread utility in crystal engineering⁴ mainly because of their increased availability through organic synthesis (e.g., Arbuzov or Mannich reactions).⁵ Metal phosphonate materials are commonly coordination polymers, occasionally exhibiting microporous properties.⁶ Features that are sought in such functional materials are intercalation,⁷

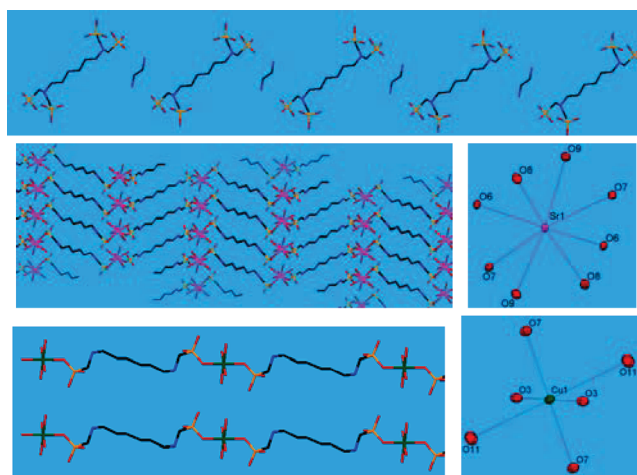


Figure 1. Structure of $(\text{en})(\text{HDTMP})$ (upper). Zigzag chains and Sr/Ba-bicapped octahedral coordination in $(\text{Sr}, \text{Ba})\text{-HDTMP}$ (**1**, **2**; middle). Linear chains and Cu “Jahn–Teller”-distorted octahedral coordination in Cu-HDTMP (**3**; lower). “Dangling”, noncoordinated phosphonate groups are omitted for clarity.

catalysis,⁸ sorption and storage,⁹ and ion exchange.¹⁰ Hydrogen bonds are predominant and usually responsible for the stabilization of such architectures resulting in one-, two-, and three-dimensional supramolecular networks.

Phosphonate additives have been extensively tested as inhibitors for scale inhibition^{11a} and metallic corrosion protection.^{11b} There is a consensus in literature reports on a synergistic action of dissolved M^{2+} ($M = \text{usually an alkaline-earth metal or Zn}$) and polyphosphonates that is explained on the basis of inhibiting metal phosphonate film formation on the metallic surface.¹² However, little is known about the molecular structure of these inhibiting films. Recently, we initiated a

* To whom correspondence should be addressed. E-mail: demadis@chemistry.uoc.gr. URL: www.chemistry.uoc.gr/demadis.

[†] Present address: Department of Chemistry, University of Puerto Rico at Rio Piedras, San Juan, Puerto Rico.

[‡] Present address: Ordered Matter Science Research Center, Southeast University, Nanjing, People's Republic of China.

(1) (a) Kitagawa, S.; Kitaura, R.; Noro, S. *Angew. Chem., Int. Ed.* **2004**, *43*, 2334. (b) Wang, Z.; Kravtsov, V. C.; Zaworotko, M. J. *Angew. Chem., Int. Ed.* **2005**, *44*, 2877.

(2) Bauer, S.; Stock, N. *Angew. Chem., Int. Ed.* **2007**, *46*, 6857.

(3) Forster, P. M.; Stock, N.; Cheetham, A. K. *Angew. Chem., Int. Ed.* **2005**, *44*, 7608.

(4) Kong, D.; Clearfield, A.; Zon, J. *Cryst. Growth Des.* **2005**, *5*, 1767.

(5) Mikolajczyk, M.; Balczewski, P. *Top. Curr. Chem.* **2003**, *223*, 162.

(6) Taylor, J. M.; Mahmoudkhani, A. H.; Shimizu, G. K. H. *Angew. Chem., Int. Ed.* **2007**, *46*, 795.

(7) Williams, G. R.; Norquist, A. J.; O'Hare, D. *Chem. Commun.* **2003**, 1816.

(8) Clearfield, A. *J. Mol. Catal.* **1984**, *27*, 251.

(9) (a) Groves, J. A.; Miller, S. R.; Warrender, S. J.; Mellot-Draznieks, C.; Lightfoot, P.; Wright, P. A. *Chem. Commun.* **2006**, 3305. (b) Miller, S. R.; Pearce, G. M.; Wright, P. A.; Bonino, F.; Chavan, S.; Bordiga, S.; Margiolaki, I.; Guillou, N.; Férey, G.; Bourrelly, S.; Llewellyn, P. L. *J. Am. Chem. Soc.* **2008**, *130*, 15967.

(10) Alberti, G.; Casciola, M. *Solid State Ionics* **2001**, *145*, 3.

(11) (a) Barouda, E.; Demadis, K. D.; Freeman, S.; Jones, F.; Ogden, M. I. *Cryst. Growth Des.* **2007**, *7*, 321. (b) Demadis, K. D. In *Solid State Chemistry Research Trends*; Buckley, R. W., Ed.; Nova Science Publishers: New York, 2007; p 109.

(12) Marin-Cruz, J.; Cabrera-Sierra, R.; Pech-Canul, M. A.; Gonzalez, I. *Electrochim. Acta* **2006**, *51*, 1847.

systematic effort in delineating the mechanisms of metal phosphonate films on metal surfaces, focusing on their accurate description at the molecular level.¹³

Herein, we describe the syntheses¹⁴ of five novel divalent metal tetraphosphonates, M-HDTMP [$M = \text{Mg}^{2+}$, Ca^{2+} , Sr^{2+} , Ba^{2+} , and Cu^{2+} ; HDTMP = hexamethylenediaminetetrakis-(methylenephosphonate) dianion]. Compounds $\{\text{Sr}[(\text{HDTMP})\cdot(\text{H}_2\text{O})_6]\cdot 2\text{H}_2\text{O}\}_n$ (**1**), $\{\text{Ba}[(\text{HDTMP})(\text{H}_2\text{O})_6]\cdot 2\text{H}_2\text{O}\}_n$ (**2**), and $\{\text{Cu}[(\text{HDTMP})(\text{H}_2\text{O})_4]\cdot 6\text{H}_2\text{O}\}_n$ (**3**), as well as $(\text{en})(\text{HDTMP})\cdot 2\text{H}_2\text{O}$ ($\text{en} = \text{ethylenediammonium cation}$) were structurally characterized.¹⁵ Crystal structures depend on the coordination

requirements of the M^{2+} center and waters of crystallization content. The formation and characterization of anticorrosion passive films of M-HDTMP ($M = \text{Sr}^{2+}$ and Ba^{2+}) are also described.

Reactions of water-soluble M^{2+} ($M = \text{Mg}$, Ca , Sr , Ba , and Cu) inorganic salts with HDTMP yield single-phase products [based on powder X-ray diffraction (XRD) patterns, except the Cu-HDTMP system, which yields multiple phases], with varying amounts of coordinated and lattice waters (see the Supporting Information). The structure of $(\text{en})(\text{HDTMP})\cdot 2\text{H}_2\text{O}$ (Figure 1) is composed of discrete en^{2+} and HDTMP^{2-} ions and dominated by hydrogen bonds between $-\text{NH}_3^+$ (from en^{2+}) and phosphonate groups (from HDTMP^{2-}), and the two lattice waters. All M-HDTMP compounds have a one-dimensional chain structure. The isostructural M-HDTMP [$M = \text{Sr}$ (**1**), Ba (**2**); Figure 1] compounds form a zigzag, corrugated arrangement with an “opening” angle of $\text{P}(\text{O})-\text{M}-\text{O}(\text{P})$ of $115.59(9)^\circ$ (for Sr) and $117.66(8)^\circ$ (for Ba). The coordination environment of the eight-coordinated Sr^{2+} (Ba^{2+}) center in **1** (**2**) can be described as a bicapped octahedron. The $\text{M}-\text{M}-\text{M}$ angles are very similar, $150.3(2)^\circ$ for **1** and $149.7(2)^\circ$ for **2**. The Cu-HDTMP (**3**) compound is one-dimensional, and in contrast to compounds **1** and **2**, the $\text{Cu}\cdots\text{Cu}\cdots\text{Cu}$ “chain” is linear. The Cu^{2+} center is six-coordinated.

The Jahn–Teller effect is profoundly demonstrated in the $\text{Cu}-\text{O}(\text{H}_2\text{O})$ bond distances; two are $1.9672(19)$ Å and the other two $2.434(3)$ Å. All three structures share a common structural feature that two phosphonate arms (one from each N) are not metal-coordinated but are “dangling” and participate in hydrogen bonds with neighboring $-\text{PO}_3\text{H}^-$ moieties and H_2O molecules. Only three other M-HDTMP structures (very different from **1–3**) are available in the literature with Zn ,^{13a} Co ^{16a} and Cu .^{16b} Thermogravimetric analysis studies showed that there is a major loss at $\sim 116^\circ\text{C}$ ($\sim 16.2\%$ for **1** and $\sim 12.9\%$ for **2**; see the Supporting Information). This loss corresponds to ~ 6.5 molecules of H_2O for **1** or **2**. Above 400°C , both compounds undergo loss that corresponds to all eight molecules of water for **1** and **2**.

Corrosion experiments were performed¹⁷ in order to study the nature of the protective anticorrosion coating. Corrosion inhibitory activity was based on mass loss measurements.¹⁷ The effectiveness of corrosion protection by synergistic combinations of M^{2+} and HDTMP, in a 1:1 ratio is dramatically pH-dependent (Table 1 and Figure 2). At “harsh” pH regions (~ 2.2), mass loss from the steel specimens is profound, resulting in high corrosion rates. However, specimens **2** and **3** (Figure 2) appear free of corrosion products, presumably because HDTMP (either free or metal-bound) at the surface acts as an iron oxide dissolving agent. We have observed a similar behavior in

- (13) (a) Demadis, K. D.; Mantzaridis, C.; Raptis, R. G.; Mezei, G. *Inorg. Chem.* **2005**, *44*, 4469. (b) Demadis, K. D.; Lykoudis, P.; Raptis, R. G.; Mezei, G. *Cryst. Growth Des.* **2006**, *6*, 1064.
- (14) All starting materials are commercial. HDTMP was from Solutia Inc. It was also synthesized by a Mannich-type reaction (Princz, E.; Szilágyi, I.; Mogyorósi, K.; Labádi, I. *J. Therm. Anal. Calorim.* **2002**, *69*, 427.). Syntheses either at room temperature or hydrothermal, with either commercial or in-house-synthesized HDTMP, have yielded identical results. $(\text{en})(\text{HDTMP})\cdot 2\text{H}_2\text{O}$ was obtained from failed attempts to synthesize Zn-HDTMP materials but can also be prepared from HDTMP and en. The Zn^{2+} ion was not incorporated into the final product. A quantity of acid HDTMP (1.230 g, 2.5 mmol) is suspended in 40 mL of deionized water and mixed with 1.2 mL of en (neat). Then a quantity of $\text{ZnCl}_2\cdot 6\text{H}_2\text{O}$ is added (0.204 g, 1.5 mmol) under rigorous stirring, and the final pH is adjusted to 2.5, yielding a clear colorless solution. After standing under quiescent conditions for 2 days, colorless crystals appear, which are isolated by filtration, washed with deionized water, and air-dried. Yield $\sim 40\%$. M-HDTMP compounds are prepared with identical procedures. Quantities of a hydrated metal chloride (2.32 mmol) and HDTMP (4 mL of a 50% solution of $\text{Na}_4\text{-HDTMP}$, 2.32 mmol) are mixed in deionized water (~ 40 mL) under vigorous stirring. The solution pH is adjusted to 2.2 by use of either HCl or NH_4OH solutions, as needed. Crystals form within days from the clear, colorless solutions, but crystallization is allowed to proceed further. Syntheses were repeated at pH ~ 7 for the Sr- and Ba-HDTMP compounds, and products were treated as above. Precipitation is more rigorous at higher pH, and products are amorphous by XRD. Yields range from 50% to 70% depending on crystallization time. Satisfactory elemental analyses were obtained for all products, except Cu-HDTMP (**3**), whose synthesis yields more than one phase. FT-IR spectra of M-HDTMP products display a multitude of bands in the region $950\text{--}1200\text{ cm}^{-1}$ assigned to the $\text{P}=\text{O}$ stretch. Further details on syntheses and spectroscopic characterization are given in the Supporting Information.
- (15) Crystal data were collected on a SMART 1K CCD diffractometer at $293(2)$ K with $\text{Mo K}\alpha$ ($\lambda = 0.71073$ Å). **(en)(HDTMP)**: colorless cubic blocks ($0.22 \times 0.20 \times 0.16$ mm), triclinic, space group $P\bar{1}$, with $a = 6.1950(11)$ Å, $b = 7.4889(13)$ Å, $c = 15.955(3)$ Å, $\alpha = 84.472(3)^\circ$, $\beta = 85.319(3)^\circ$, $\gamma = 67.881(3)^\circ$, $V = 681.7(2)$ Å³, and $Z = 2$, $d_{\text{calcd}}/\text{g cm}^{-3} = 1.511$, total reflections 4795, refined reflections [$I_{\text{net}} > 2\sigma(I_{\text{net}})$] 3056, number of parameters 176, $R_1 = 0.0566$ (0.0711, all data), $wR_2 = 0.1614$ (0.1691, all data), $\text{GOF} = 1.073$. **Sr-HDTMP (1)**: colorless rectangular plates ($0.26 \times 0.23 \times 0.04$ mm), monoclinic, space group $C2/c$, with $a = 13.999(4)$ Å, $b = 5.9939(13)$ Å, $c = 33.447(12)$ Å, $\beta = 101.52(2)^\circ$, $V = 2750.1(14)$ Å³, and $Z = 4$, $d_{\text{calcd}}/\text{g cm}^{-3} = 1.744$, total reflections 16177, refined reflections [$I_{\text{net}} > 2\sigma(I_{\text{net}})$] 1932, number of parameters 182, $R_1 = 0.0365$ (0.0375, all data), $wR_2 = 0.1032$ (0.1037, all data), $\text{GOF} = 1.141$. **Ba-HDTMP (2)**: colorless rectangular plates ($0.22 \times 0.18 \times 0.10$ mm), monoclinic, space group $C2/c$, with $a = 14.084(4)$ Å, $b = 6.0158(15)$ Å, $c = 33.793(9)$ Å, $\beta = 100.717(4)^\circ$, $V = 2813.3(12)$ Å³, and $Z = 4$, $d_{\text{calcd}}/\text{g cm}^{-3} = 1.822$, total reflections 8568, refined reflections [$I_{\text{net}} > 2\sigma(I_{\text{net}})$] 2982, number of parameters 175, $R_1 = 0.0345$ (0.0361, all data), $wR_2 = 0.0905$ (0.0913, all data), $\text{GOF} = 1.281$. **Cu-HDTMP (3)**: light blue needles ($0.18 \times 0.08 \times 0.05$ mm) were manually selected from the bulk, triclinic, space group $P\bar{1}$, with $a = 6.267(2)$ Å, $b = 7.6810(12)$ Å, $c = 16.879(7)$ Å, $\alpha = 86.36(3)^\circ$, $\beta = 83.74(2)^\circ$, $\gamma = 66.44(2)^\circ$, $V = 740.1(4)$ Å³, and $Z = 1$, $d_{\text{calcd}}/\text{g cm}^{-3} = 1.647$, total reflections 4540, refined reflections [$I_{\text{net}} > 2\sigma(I_{\text{net}})$] 2457, number of parameters 230, $R_1 = 0.0324$ (0.0399, all data), $wR_2 = 0.0848$ (0.0876, all data), $\text{GOF} = 1.033$. CCDC codes: $(\text{en})(\text{HDTMP})\cdot 2\text{H}_2\text{O}$, 651135; **1**, 291524; **2**, 293464; **3**, 605562.

- (16) (a) Zheng, G.-L.; Ma, J.-F.; Yang, J. *J. Chem. Res.* **2004**, 387. (b) Costantino, F.; Bataille, T.; Audebrand, N.; Le Fur, E.; Sangregorio, C. *Cryst. Growth Des.* **2007**, *7*, 1881.

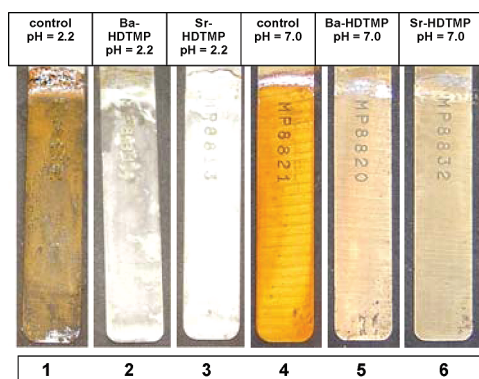
- (17) Corrosion protocol: NACE Standard TM0169-95 (item no. 21200). Herein some protocol details pertinent to this study are provided. Specimens (carbon steel C1010 from Metal Samples Corrosion Monitoring Systems, Munford, AL) were immersed in a “control” (no inhibitor) or in a “test” solution (100 mL), containing Sr^{2+} or Ba^{2+} and HDTMP in a 1:1 molar ratio, at various levels (Table 1). The pH (2.2 or 7.0) was adjusted by the addition of a HCl or NH_4OH solution. Corrosion rates are determined after 5 days from mass loss measurements; see the protocol above.

Table 1. Corrosion Rates and Percent Inhibition^a Obtained in the Absence (Control) and Presence of HDTMP or M²⁺-HDTMP Combinations^b

M-HDTMP compound	additive concentration (mM) ^c	corrosion rate (CR, mm/year)	
		pH 2.2	pH 7.0
control	no additives	2.435	0.682
HDTMP	0.5	1.863	23.5% inhibition
	0.8	2.387	metal dissolution
	1.5	3.129	metal dissolution
Sr-HDTMP	0.5	3.060	metal dissolution
	0.8		0.234 65.7% inhibition
	1.0	2.181	10.3% inhibition
	1.5		1.152 metal dissolution ^d
Ba-HDTMP	0.5	3.053	metal dissolution
	0.8		0.093 86.4% inhibition
	1.0	2.888	metal dissolution
	1.5		0.097 85.8% inhibition

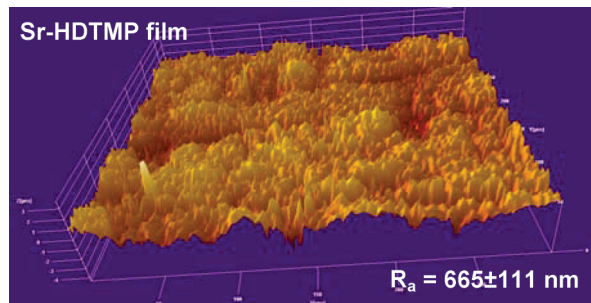
^a Percent inhibition is defined as $[(CR_{\text{control}} - CR_{\text{inhibitor}})/CR_{\text{control}}] \times 100$.

^b The corrosion rate is calculated from the equation $CR = [534.57(\text{mass loss})]/[(\text{area})(\text{time})(\text{metal density})]$. Units: CR in mm/year, mass loss in mg, area in cm², time in h, metal density = 7.85 g/cm³. ^c The concentration refers to [M²⁺] and [HDTMP] that are added in a 1:1 molar ratio. ^d The ineffectiveness of a Sr-HDTMP film at higher [Sr²⁺] and [HDTMP] may be due to bulk precipitation of the Sr-HDTMP (1) compound before reaching the steel surface.

**Figure 2.** Anticorrosive effect of M-HDTMP films on carbon steel. The effect of M-HDTMP synergistic combinations is dramatically demonstrated (specimens 2, 3, 5, and 6).

corrosion experiments with M²⁺ (Ca or Zn) and phosphonobutane-1,2,4-tricarboxylic acid.^{13b} At pH 7.0, corrosion rates are appreciably suppressed (Table 1) in the presence of combinations of Sr²⁺ or Ba²⁺ and HDTMP (specimens 5 and 6). Corrosion rates are concentration-dependent for Sr-HDTMP, whereas they are insensitive to Ba-HDTMP levels.¹⁸

However, when HDTMP (without M²⁺ ions) is used at pH 7.0, corrosion rates increase, apparently because of the increased iron oxide dissolving ability of the further deprotonated HDTMP (Table 1). The corrosion specimens (at pH 7.0) and film material were subjected to studies by vertical scanning interferometry (VSI; Figure 3), scanning electron microscopy (SEM), FT-IR, X-ray fluorescence, energy-dispersive spectrometry, and X-ray photoelectron spectroscopy in order to characterize the protective coating. Most data are found in the Supporting Information. Data show that at pH 2.2 (ineffective protection) the only material identified on the steel specimens was an amorphous (by XRD) Fe-HDTMP compound. Both Sr²⁺ and Ba²⁺ were absent. At pH 7.0, the inhibiting film (see Figure 3 and SEM in the Supporting Information) is fairly uniform and contains M²⁺ (Sr or Ba from externally added salts) and P (from added HDTMP), in an approximate 1:2 molar ratio, suggesting a ratio of two Sr (Ba) cations and one HDTMP ligand. FT-IR of the

**Figure 3.** Anticorrosion film morphology viewed by VSI. The grid size is $9 \times 10^4 \mu\text{m}^2$. The height of the z axis is $3 \mu\text{m}$. R_a is the average surface roughness, or average deviation, of all points from a plane fit to the test part of the surface.

filming material showed multiple bands associated with the phosphonate groups in the $950\text{--}1200 \text{ cm}^{-1}$ region that closely match those of authentically prepared M-HDTMP salts at pH 7.0 (see the Supporting Information).

In order to gain further insight on the M-HDTMP inhibiting films at pH 7.0, syntheses of M-HDTMP compounds were pursued at pH 7.0 for Sr and Ba. Amorphous solids were obtained in all cases that showed characteristic bands for metal-coordinated phosphonate groups, and their FT-IR spectra matched perfectly with those of the protective films (see the Supporting Information). Their elemental analyses were consistent with the formulas $\{M_2[(\text{HDTMP})(\text{H}_2\text{O})_{12}]\}_n$ ($M = \text{Sr}$ and Ba). In turn, these formulas are consistent with a second metal site being coordinated by two “dangling” phosphonate oxygen atoms (from two neighboring “chains”) along with six H₂O molecules. Such a hypothetical structure would lead to a ladder-type architecture. The formation of Cu-HDTMP on carbon steel is not possible because of immediate Cu²⁺ reduction to Cu⁰ metal with concomitant Cu plating of the steel specimen.¹⁹

Herein we reported syntheses and structural characterization of divalent M-HDTMP ($M^{2+} = \text{Sr}$, Ba , and Cu) coordination polymers. When generated in situ, they act as corrosion inhibitors at circumneutral pH by creating anticorrosive protective films on a steel surface. Although the field of metal phosphonate chemistry is rather mature, there is still a plethora of opportunities in basic research and industrially significant application areas.

Acknowledgment. We thank the GSRT and University of Crete Special Research Account (ELKE) for funding (Project KA 2573) and Dr. V. Ramos for technical assistance.

Supporting Information Available: Full details of the synthesis and characterization and also CIF files. This material is available free of charge via the Internet at <http://pubs.acs.org>.

IC802032Y

- (18) Variation in the corrosion rates could be linked to different HDTMP complex formation constants for Sr²⁺ and Ba²⁺. Such data are unavailable. Similar formation constants (7.10–7.56) have been reported for a “shorter” tetraphosphonate, EDTMP. See Sawada, K.; Miyagawa, T.; Sakaguchi, T.; Doi, K. *J. Chem. Soc., Dalton Trans.* **1993**, 3777. Thus, differences observed in the corrosion rates may be due to the physical stability of the M-HDTMP anticorrosion film.
- (19) When a Cu specimen comes in contact with a solution of free HDTMP (~1.0 mM), higher corrosion rates (0.469 mm/year) than those for the control (0.131 mm/year) are observed. Apparently, Cu metal oxidation/dissolution occurs with concomitant formation of Cu-HDTMP, shown by FT-IR (see the Supporting Information).